

## **$\gamma$ -Secretase/presenilin inhibitors for Alzheimer's disease phenocopy *Notch* mutations in *Drosophila***

Craig A. Micchelli<sup>\*</sup>, William P. Esler<sup>†</sup>, W. Taylor Kimberly<sup>†</sup>, Christine Jack<sup>‡</sup>, Oksana Berezovska<sup>‡</sup>, Anna Kornilova<sup>†</sup>, Bradley T. Hyman<sup>‡</sup>, Norbert Perrimon<sup>\*</sup>, and Michael S. Wolfe<sup>†</sup>

<sup>\*</sup>Department of Genetics, Howard Hughes Medical Institute, Harvard Medical School, Boston, MA 02115; <sup>†</sup>Center for Neurologic Diseases, Harvard Medical School, Brigham and Women's Hospital, Boston, MA 02115; <sup>‡</sup>Alzheimer's Disease Research Laboratory, Department of Neurology, Harvard Medical School, Massachusetts General Hospital, Charlestown, MA 02129, USA

Corresponding author: Michael S. Wolfe, Center for Neurologic Diseases, Brigham and Women's Hospital, 77 Avenue Louis Pasteur, H.I.M. 626, Boston, Massachusetts 02115. E-mail: mwolfe@rics.bwh.harvard.edu

### **ABSTRACT**

Signaling from the Notch (N) receptor is essential for proper cell-fate determinations and tissue patterning in all metazoans. N signaling requires a presenilin (PS)-dependent transmembrane-cleaving activity that is closely related or identical to the  $\gamma$ -secretase proteolysis of the amyloid- $\beta$  precursor protein (APP) involved in Alzheimer's disease pathogenesis. Here, we show that *N*-[*N*-(3,5-difluorophenacetyl)-L-alanyl]-(*S*)-phenylglycine *t*-butyl ester, a potent  $\gamma$ -secretase inhibitor reported to reduce amyloid- $\beta$  levels in transgenic mice, prevents N processing, translocation, and signaling in cell culture. This compound also induces developmental defects in *Drosophila* remarkably similar to those caused by genetic reduction of *N*. The appearance of this phenocopy depends on the timing and dose of compound exposure, and effects on *N*-dependent signaling molecules established its biochemical mechanism of action *in vivo*. Other  $\gamma$ -secretase inhibitors caused similar effects. Thus, the three-dimensional structure of the drug-binding site(s) in *Drosophila*  $\gamma$ -secretase is remarkably conserved vis-à-vis the same site(s) in the mammalian enzyme. These results show that genetics and developmental biology can help elucidate the *in vivo* site of action of pharmacological agents and suggest that organisms such as *Drosophila* may be used as simple models for *in vivo* prescreening of drug candidates.

Key words: protease • developmental biology • drug screening

**G**enetic manipulation is commonly used to modulate specific protein function and signaling pathways to explore their role in development. In contrast, studies demonstrating comparable pharmacological modulation of specific pathways during development are rare. In one striking example, however, veratrum alkaloids such as cyclopamine are teratogens that induce cyclopia and other birth defects in vertebrates,

apparently by interfering with the ability of cells to respond to Sonic hedgehog, a secreted protein that is part of a highly conserved signaling pathway essential for metazoan development (1). Moreover, the transforming effects of oncogenic mutations in two members of the hedgehog signaling pathway, *smoothened* and *patched*, can be reversed by cyclopamine (2). In another example, an inhibitor of Ras farnesylation representative of a class of potential anticancer agents did not appear to affect normal *Drosophila* development; however, this compound could reduce the ability of oncogenic Ras to form extra photoreceptors (3). These illustrations show that pathways critical for development can cause human disease and that pharmacological agents that modulate these pathways can be both useful experimental tools and potential therapeutic agents.

The N signaling pathway is likewise highly conserved (4), essential for proper metazoan development (5), and implicated in human disease. N is involved in a variety of cell-lineage determinations, and aberrant N signaling can cause cancer (e.g., leukemias) (6), neurological disease (CADASIL) (7), and developmental abnormalities (Alagille syndrome) (8, 9). After binding to its cognate ligand, N is processed sequentially by two proteases, tumor necrosis factor- $\alpha$  converting enzyme (TACE) (10) and the presenilin (PS)-dependent  $\gamma$ -secretase (11). Proteolysis by  $\gamma$ -secretase occurs within the transmembrane region of N and allows the N intracellular domain (NICD) to translocate to the nucleus where it regulates the transcription factor Lag1/Su(H)/CBF1 (Fig. 1a) (12). A similar or identical  $\gamma$ -secretase activity processes the transmembrane region of the APP, the final step in the production of the amyloid- $\beta$  protein (A $\beta$ ; Fig. 1a) that is implicated in the etiology of Alzheimer's disease (13).

Pharmacological profiling, site-directed mutagenesis, biochemical analysis, and affinity labeling strongly suggest that  $\gamma$ -secretase is an aspartyl protease and that the multi-pass PS is the catalytic component of the  $\gamma$ -secretase complex (Fig. 1a) (13). Because of its role in A $\beta$  production,  $\gamma$ -secretase is considered an important target for the prevention and treatment of AD, and several potent and specific inhibitors of the  $\gamma$ -secretase cleavage of APP are known (14). Several  $\gamma$ -secretase inhibitors have been shown to block the transmembrane cleavage of N (11, 15) and subsequent nuclear translocation and signaling (16) in cell culture. Here, we report that *N*-[*N*-(3,5-difluorophenacetyl)-L-alanyl]-(*S*)-phenylglycine *t*-butyl ester (DAPT), a compound developed to lower A $\beta$  levels *in vivo* as a potential treatment for Alzheimer's disease (17), blocks N proteolysis and signaling in cell culture and induces *N*-deficient developmental defects in *Drosophila*. These findings demonstrate that the three-dimensional structure of the drug-binding site on  $\gamma$ -secretase is conserved between mammals and *Drosophila*.

## MATERIALS AND METHODS

### Compounds and inhibition of $\gamma$ -secretase activity

DAPT and compound E were synthesized as previously reported (17, 18), and WPE-III-63 was prepared using methods previously described (19, 20). Solubilized  $\gamma$ -secretase was prepared from HeLa cells as described by Li et al. (21), except that membranes were washed in 0.1 M sodium carbonate (pH 11.3) before solubilization in CHAPSO. The solubilized

preparation (at ~200 µg of protein per mL) was incubated with Flag-tagged substrate C100Flag or N100Flag and analyzed for Aβ or Flag-tagged proteolytic product, respectively, as previously described (20, 21).

### **Photoaffinity labeling**

Irradiation of solubilized microsomes treated with WPE-III-63 and precipitation with streptavidin-agarose beads were performed essentially as described previously using a close structural analog (22). After sodium dodecyl sulfate-polyacrylamide gel electrophoresis (SDS-PAGE) and transfer to PVDF, membranes were probed with polyclonal antibody Ab14 to the PS1 N-terminus and monoclonal antibody 13A11 to the PS1 C-terminus and visualized using anti-rabbit or anti-mouse IgG-HRP.

### **N-GFP translocation and luc reporter assay**

Determination of NICD translocation and signaling from a luciferase reporter were performed in CHO cells as previously described (16) using cDNA encoding NotchΔE-EGFP, a truncated form of human Notch1 lacking the ectodomain and tagged at the C-terminus with EGFP.

### **Fly strains used and compound treatments**

Fly strains used were wild-type Oregon R (OreR); *neu-lacZ*; *vg* intron 2- *lacZ* (kindly provided by Sean Carroll);  $N^{55e11}$  FRT<sup>18A</sup>; TM3 *Ser*. Stock solutions of 50 mM compound in ethanol were added to 3 mL of water to the desired final concentration (<2% ethanol), and dried potato food was mixed in to the consistency of mashed potatoes. Vials were kept overnight to allow evaporation of residual ethanol. Into each vial, 10 females and 5 males were introduced and kept at 25°C for 5 days. Adults were removed, and progeny were allowed to progress in the presence of compound until eclosion. For timing experiments, eggs collected over a 2-h period were collected and treated in two ways: 1) Eggs were added to vials containing food mixed with DAPT. After 48–120 h, larvae were moved into fresh vials containing food alone. 2) Eggs were added to vials containing food alone. After 48–120 h, larvae were moved into fresh vials containing food mixed with DAPT.

### **Immunohistochemistry**

Wing imaginal discs were dissected from late third instar larvae in *Drosophila* Ringers solution and fixed in cold 2% formaldehyde and Browsers buffer overnight at 4°C. Discs were washed in phosphate-buffered saline (PBS) T buffer for at least 2 h before incubation with primary antibodies (mouse anti-Ct [2B10, Developmental Studies Hybridoma Bank, University of Iowa, Iowa City], 1:10; mouse anti-Wg [4D4, Developmental Studies Hybridoma Bank], 1:10; and rabbit anti-β-galactosidase [ICN/Cappel, Aurora, OH], 1:2000). All fluorescent secondary (low cross reactivity, Jackson ImmunoResearch (West Grove, PA)) antibodies were used at 1:200. Primary antibodies were detected using fluorescent secondary antibodies or the nickel-intensified Vector (Burlingame, CA) ABC-DAB kit (for a detailed protocol, see ref 23).

## RESULTS

### **DAPT inhibits N proteolysis, nuclear translocation, and signaling and blocks affinity labeling of PS**

Incubation of the recombinant APP-based substrate C100Flag with microsomes isolated from HeLa cells and solubilized with the zwitterionic detergent CHAPSO leads to  $\gamma$ -secretase-mediated production of A $\beta$  (21). DAPT blocked A $\beta$  production in this assay with an IC<sub>50</sub> of 5–10 nM (Fig. 1b), consistent with its ability to block A $\beta$  production from APP-transfected cells (17). We have recently developed an *in vitro* assay for the PS-dependent proteolysis of N, using a recombinant substrate that represents 99 residues of murine Notch1 (including the transmembrane region), an N-terminal methionine translation start site, and a C-terminal Flag epitope (N100Flag) (20). After incubation of this substrate with solubilized HeLa cell microsomes for 4 h at 37°C, a new band appears upon Western blotting (Fig. 1c, lane 1). This protein is 2–3 kDa smaller than N100Flag, consistent with what would be expected for proteolysis within the transmembrane region. This proteolytic activity in the solubilized microsomes is associated with PS, because it can be immunoprecipitated with antibodies to the N-terminus of either human PS1 (20) or PS2 (unpublished results). Moreover, the N100Flag proteolysis is blocked by a variety of inhibitors of the APP-cleaving  $\gamma$ -secretase activity (W.T.K., W.P.E., D.J. Selkoe, M.S.W.; unpublished results). We found that DAPT also inhibits proteolysis of N100Flag, with an IC<sub>50</sub> of 5–10 nM (Fig. 1c), providing further evidence that the proteases responsible for hydrolyzing the transmembrane regions of APP and N are closely similar or identical.

After transmembrane cleavage of N, the NICD translocates to the nucleus, where it activates Lag1/HES/CBF1-mediated transcription. A truncated form of N lacking the ectodomain (Notch $\Delta$ E) is constitutively cleaved by a PS-dependent  $\gamma$ -secretase activity. Transfection of CHO cells with cDNA encoding a Notch $\Delta$ E-EGFP fusion protein allows visualization of EGFP fluorescence in the nucleus (Fig. 2a), and this nuclear fluorescence was inhibited by DAPT at concentrations that also blocked cell-free proteolysis of C100Flag and N100Flag (Fig. 2a, 2b). DAPT also reduced signaling from a luciferase reporter activated by released NICD (Fig. 2c). Concentrations necessary to inhibit N signaling in this assay were higher than those capable of lowering N100Flag proteolysis or NICD translocation, consistent with a previous report that NICD produced in this signaling assay is in excess of what is needed for full signaling (16).

We have previously shown through pharmacological profiling with transition-state analog inhibitors that  $\gamma$ -secretase displays characteristics of an aspartyl protease (24). Moreover, we found through mutagenesis that two conserved transmembrane aspartates in PS are critical for  $\gamma$ -secretase processing, suggesting that these are the catalytic residues of the protease (25, 26). We and others have shown that transition-state analog  $\gamma$ -secretase inhibitors bind directly to both components of a processed, heterodimeric form of PS (22, 27). This finding strongly suggests that the active site of  $\gamma$ -secretase lies at the interface of these two subunits of PS, each of which contributes one of the critical aspartates (see Fig. 1a). Compound WPE-III-63, a transition-state analog  $\gamma$ -secretase inhibitor, contains a C-terminal biotin and a

photoactivatable P2' residue (benzoylphenylalanine) (Fig. 2d). This compound crosslinks both the NTF and CTF subunits of PS1 in a manner similar to that reported for a structurally related analog (22). DAPT prevented this affinity labeling of PS1 by WPE-III-63 (Fig. 2d), suggesting that this compound either directly binds to the active site of PS or alters the active site (e.g., through an allosteric interaction).

### **DAPT induces wing defects in developing *Drosophila* similar to genetic mutations in the *N* signaling pathway**

*N* signaling in *Drosophila* requires a highly conserved PS-dependent  $\gamma$ -secretase activity (28, 29). Reductions in either *N* or *PS* function along the presumptive wing margin of *Drosophila* leads to loss of wing margin structures in the adult (28, 30). We therefore tested whether treatment with the PS/ $\gamma$ -secretase inhibitor DAPT could cause developmental defects in flies similar to those caused by genetic reduction of *N* signaling. Adult wild-type flies were introduced into vials with food containing DAPT at concentrations ranging from 100  $\mu$ M to 1.0 mM. The adults were kept at 25°C and allowed to lay eggs over the course of 5 days. During this time, no overt toxicity was associated with DAPT. However, we did not quantify the long-term effects of the compound on fertility or viability of the adult flies. Progeny began to eclose 10 days after the introduction of the parental flies. These offspring displayed a dose-sensitive wing notching phenotype that was indistinguishable from genetic reductions in the *N* pathway (cf., Fig. 3a–g). Defects in wing development first became evident at 500  $\mu$ M of DAPT; however, at this concentration, the wing notching phenotype was not fully penetrant. At 1 mM of DAPT, virtually all of the progeny displayed defective wings (Fig. 3i). These ranged in severity from a mild to strong wing notching phenotype (Fig. 3a–g). F2 progeny derived from the defective DAPT-treated F1 flies had wild-type wings, demonstrating that the effect of DAPT on wing development is not due to a genetic alteration.

We also noted that DAPT-treated flies displayed several additional phenotypes consistent with defects in *N* signaling. These include an increased number of bristles on the notum, defects in leg segmentation, and small eyes (Fig. 3j, 3k and data not shown), but these were only observed at a low frequency. Thus, DAPT was not able to fully mimic the effects of reducing *N* function (31). Moreover, DAPT also caused some lethality at concentrations that caused almost full penetrance of the wing phenocopy (500  $\mu$ M and 1 mM). There are several possible explanations for these observations. These include the particular pharmacokinetic properties (e.g., uptake, metabolism, and distribution) of DAPT in flies, the genetic background, and the documented requirements of *N* for viability (31). In addition, this compound may cause other types of toxicities not related to interference with *N* signaling.

In a control experiment, we introduced flies into vials with food containing *N*-(3,5-difluorophenacetyl)-L-alanine *t*-butyl ester (DAT). DAT is identical to DAPT except that it does not contain the phenylglycine residue and is inactive against  $\gamma$ -secretase up to 1  $\mu$ M in the cell-free N100Flag assay (data not shown). In contrast to DAPT, DAT treatment did not elicit any identifiable defects (Fig. 3h, 3j). Thus, the phenotypes that result from DAPT treatment are unlikely to be an artifact of the experimental conditions themselves, but rather a direct consequence of DAPT's ability to inhibit  $\gamma$ -secretase activity.



Analysis of a temperature-sensitive allele of *N* has demonstrated that *N* is required during the third larval instar for wing margin development (31). We therefore asked when during development DAPT caused its effects on wing formation. To address this issue, we conducted two different experiments. In the first experiment, embryos from wild-type flies were collected over a 2-h period and placed into food containing DAPT at 25°C. At defined intervals, larvae were transferred out of DAPT to fresh food and allowed to develop to adulthood. In the second experiment, embryos from wild-type flies were collected over a 2-h period and placed into food without DAPT at 25°C. At defined intervals, larvae were transferred onto food containing DAPT and subsequently allowed to develop to adulthood. As shown in [Figure 4a](#), among the adult flies recovered from this experiment, no effect on wing development was detected upon DAPT treatment before or after day 4 (72–96 h) of development. In both experiments, larvae exposed to DAPT between 72 and 96 h of development resulted in wing notching phenotypes. Exposing larvae to DAPT only during day 4 (72–96 h) of development was also sufficient to induce wing defects ([Fig. 4b](#)). This corresponds closely to the period in which *N* is known to be required for wing margin formation (31), suggesting that DAPT treatment mimics a mild reduction of *N* signaling during wing development.

### **Immunostaining demonstrates that DAPT blocks *N* signaling *in vivo***

By the third larval instar, several genes are known to be expressed in a narrow stripe, three to five cells wide, that marks the presumptive wing margin. These include the homeobox-containing transcription factor encoded by *cut* (*ct*) and the secreted ligand encoded by *wingless* (*wg*). Reduction or loss of *N* along the presumptive wing margin leads to loss of both *ct* and *wg* expression and to wing notching (32–34).

To determine whether the wing notching phenocopy associated with DAPT treatment was a direct consequence of reducing *N* signaling, we tested the effect of DAPT on *N* target gene expression. Third instar larvae grown on food containing 1 mM of DAPT were dissected and stained with anti-Ct and anti-Wg antisera. In comparison to untreated larvae, discs from treated larvae displayed variable effects on both Ct and Wg protein levels ([Fig. 5a–d](#)). In the most extreme cases, little or no expression of either marker could be detected along the presumptive wing margin and the wing pouch size was substantially reduced, a further indication that *N* signaling had been affected.

Although high levels of Ct and Wg along the presumptive wing margin depend on *N*, Ct and *wg* both exhibit domains elsewhere in the wing disc that are not *N*-dependent (35). For example, several sensory mother cells (SMCs) fated to give rise to neurons also express Ct and can be detected in the presumptive wing blade and hinge ([Fig. 5b](#), arrows). Similarly, Wg is expressed in two rings around the wing pouch ([Fig. 5d](#), arrows). We found that even in cases in which the loss of Ct and Wg along the margin are most severe, levels of Ct in the SMCs and Wg in the rings were not affected. These results suggest that DAPT can specifically affect *N*-dependent processes.

However, wing notching and loss of target genes along the presumptive wing margin can result either from a loss of N signaling or from a loss of wg signaling. We wanted to test the ability of DAPT to specifically disrupt N. Occasionally, we found an increase in the number of Ct-containing cells in the presumptive hinge and notum. The ectopic Ct-containing cells were detected in proneural regions, areas competent to give rise to neural precursors, suggesting that DAPT treatment also disrupted neurogenesis. To verify this, we examined the expression of *neuralized* (*neu*), the earliest known marker of the neural lineage. As with Ct, we observed an increase in the number of *neu-LacZ*-expressing cells in the presence of DAPT (cf., [Fig. 5e, 5f](#)). This phenotype is similar to the neural hyperplasia that results from a reduction in N function, although less severe (compare to [Fig. 5b](#) in ref 33). In contrast, a reduction in wg function leads to a loss of SMCs (36). The effect of DAPT treatment on neurogenesis in the wing imaginal disc suggests that DAPT exerts its effect by disrupting N but not wg signaling.

In a final test, we examined the effect of DAPT treatment on the expression of the *vestigial* (*vg*) intron-2-*LacZ* reporter ([Fig. 6](#)). Like *ct* and *wg*, *vg* intron 2 is expressed along the presumptive wing margin in a N-dependent manner (33, 37, 38). However, unlike *ct* and *wg*, *vg* intron 2 has been shown to be a direct target of Suppressor of Hairless [Su(H)], the fly orthologue of the mammalian CBF1 protein and the primary effector of N signal transduction (39). Compared with untreated controls, DAPT treatment resulted in a variable reduction of *vg* intron 2 expression along the presumptive wing margin. Thus, DAPT is sufficient to disrupt the expression of a direct transcriptional target of the N pathway.

### Other $\gamma$ -secretase inhibitors can elicit the N phenocopy

In light of the previous observations with DAPT, we also tested the benzodiazepine-containing compound E, the most potent  $\gamma$ -secretase inhibitor reported to date (18). This compound elicited wing and eye defects similar to those seen upon DAPT treatment and at lower concentrations (100–250  $\mu$ M) than DAPT. However, this compound also caused considerable lethality (very few pupae eclosed) even at concentrations that did not elicit wing defects. The observed lethality is consistent with a strong reduction in N signaling. However, as mentioned previously for DAPT, the particular effects seen with compound E may be governed by the genetic background and the drug's pharmacokinetics. Several other analogs of DAPT and of transition-state mimic WPE-III-63 were also tested, but none were as effective as DAPT in eliciting specific effects on fly development. Interestingly, DAPT is the only compound reported to be effective *in vivo*, blocking A $\beta$  production in APP transgenic mice (17). These results also demonstrate the general utility of larval feeding as a means of delivering and assaying  $\gamma$ -secretase inhibitors in *Drosophila*.

## DISCUSSION

We have demonstrated here that the  $\gamma$ -secretase inhibitor DAPT blocks N signaling and induces a N-deficient phenocopy in *Drosophila*. Other  $\gamma$ -secretase inhibitors also elicit this phenocopy. These results demonstrate the remarkable conservation of the drug binding site(s) on the enzyme complex: Pharmacological agents optimized to inhibit human  $\gamma$ -secretase also interact with the fly orthologue. The implications of these findings are threefold: 1)

pharmacological agents can be used *in vivo* for studies in developmental biology in lieu of genetic mutations, 2) developmental biology can help elucidate the *in vivo* mechanism of drug action, and 3) model organisms for developmental biology may aid evaluation of drug candidates for human use.

Genetic approaches to development are clearly invaluable, providing precise manipulations of protein expression, distribution, and identity. *In vivo* pharmacological manipulations offer an alternative, providing a simple means of conditional control without the need for generating temperature-sensitive mutants or incorporating heterologous promoters. Moreover, in cases of gene duplication, subtypes, and isoforms, pharmacological intervention allows a potential means for controlling an entire protein class, whereas the genetic approach requires modification of each gene. We have shown here that chemical treatment can be used as a surrogate for genetic manipulations in the study of developmental biology, allowing testing of penetrance and temporal requirement. Specifically, reducing N signaling with a  $\gamma$ -secretase inhibitor gave results similar to those seen using temperature-sensitive N alleles (31). Drugs and drug candidates designed for human use may affect *Drosophila* development in other cases in which the target protein, like PS, is well conserved and is thought to play a role in development.

Conversely, developmental biology can be used to determine the mechanism of drug action *in vivo*. We have illustrated this approach here, using developmental markers to determine whether DAPT blocks N signaling *in vivo*. Similar strategies could help identify the site of *in vivo* action of other compounds with unknown mechanisms. As a necessary criterion, the compound of interest must cause specific developmental defects in a model organism. Although other simple model organisms such as nematodes and zebrafish would also be amenable to this general approach, a century's worth of *Drosophila* genetics (40) makes this organism well suited for new investigations involving the interplay between developmental biology and pharmacology.

These studies also have implications for developing therapies for Alzheimer's disease and certain N-based diseases. The PS-containing  $\gamma$ -secretase complex is a major target for the design of therapeutics to treat Alzheimer's and other amyloid-related diseases (14). Whether this protease should be a target for Alzheimer's disease is currently in dispute because an apparently identical enzyme processes the N receptor as part of a critical signaling pathway in cell differentiation (11, 28, 29, 41). Thus,  $\gamma$ -secretase inhibition may result in mechanism-based toxicities, for example, by interfering with proper T-cell maturation (42, 43). However, a partial inhibition of  $\gamma$ -secretase may be sufficient to provide a therapeutic benefit through reduction of A $\beta$  levels while avoiding N-based toxicities. Interestingly, adult flies appeared to be unaffected by exposure to DAPT. Whether this is because the compound does not inhibit N processing in the adult flies or because adults are not affected by partial inhibition of N cleavage is not known from these studies. Although the effects of N loss have not been well studied in adult flies, a recent study has suggested that N loss can affect both flight and longevity (44). With respect to treating cancers associated with overactive N, blocking the  $\gamma$ -secretase proteolysis of N itself may be a worthwhile therapeutic strategy. Finding new agents that work at other points in the N signaling pathway may be beneficial in generating both drug prototypes and tools for developmental biology.



Finally, the method of pharmacological testing in *Drosophila* described here may provide a practical primary screen to identify compounds that inhibit  $\gamma$ -secretase *in vivo*. The assay is rapid, simple, and convenient: The drug candidate is mixed with fly food, then wild-type adult flies are introduced and allowed to mate and lay eggs. Within 2 wk, progeny eclose, and the resultant wing phenotype can be easily scored.  $\gamma$ -Secretase inhibitors that cause an *N* phenocopy in the fly apparently possess reasonable metabolic stability and the ability to cross biological barriers. Such compounds would therefore be more likely to access and inhibit  $\gamma$ -secretase in mammals. Further exploration of the potential of the developing fly as a model for  $\gamma$ -secretase inhibitor drug candidates is currently underway.

## ACKNOWLEDGMENTS

We thank M. Feany for advice and assistance during the early phases of this project. This work was supported in part by National Institutes of Health grants AG17574 and NS41355 to M.S.W., AG15379 to B.T.H., and a postdoctoral fellowship to C.A.M. N.P. is a Howard Hughes Medical Institute investigator.

## REFERENCES

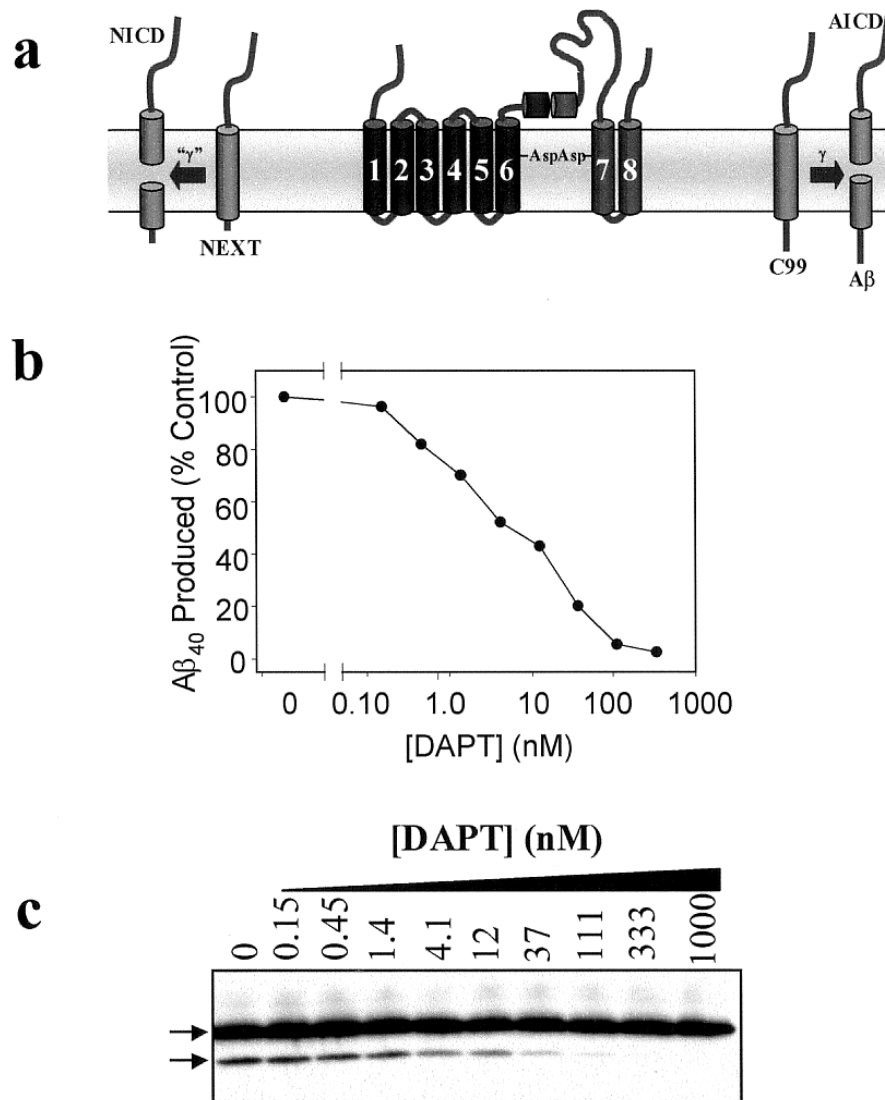
1. Cooper M. K., Porter, J. A., Young, K. E. and Beachy, P. A. (1998) *Science* **280**, 1603–1607
2. Taipale, J., Chen, J. K., Cooper, M. K., Wang, B., Mann, R. K., Milenkovic, L., et al. (2000) *Nature* **406**, 1005–1009
3. Kauffmann, R. C., Qian, Y., Vogt, A., Sebt, S. M., Hamilton, A. D. and Carthew, R. W. (1995) *Proc Natl Acad Sci USA* **92**, 10919–10923
4. Greenwald, I. (1994) *Curr Opin Genet Dev* **4**, 556–62
5. Artavanis-Tsakonas, S., Rand, M. D. and Lake, R. J. (1999) *Science* **284**, 770–776
6. Aster, J. C., and Pear, W. S. (2001) *Curr Opin Hematol* **8**, 237–244
7. Joutel, A., Corpechot, C., Ducros, A., Vahedi, K., Chabriat, H., Mouton, P., et al. (1996) *Nature* **383**, 707–710
8. Li, L., Krantz, I. D., Deng, Y., Genin, A., Banta, A. B., Collins, C. C., et al. (1997) *Nat Genet* **16**, 243–251
9. Oda, T., Elkahoul, A. G., Pike, B. L., Okajima, K., Krantz, I. D., Genin, A., et al. (1997) *Nat Genet* **16**, 235–242
10. Brou, C., Logeat, F., Gupta, N., Bessia, C., LeBail, O., Doedens, J. R., et al. (2000) *Molecular Cell* **5**, 207–216

11. De Strooper, B., Annaert, W., Cupers, P., Saftig, P., Craessaerts, K., Mumm, J. S., et al. (1999) *Nature* **398**, 518–522
12. Schroeter, E. H., Kisslinger, J. A., and Kopan, R. (1998) *Nature* **393**, 382–386
13. Esler W. P. and Wolfe M. S. (2001) *Science* **293**, 1449–1454
14. Wolfe, M. S. (2001) *J Med Chem* **44**, 2039–2060
15. Beher, D., Wrigley, J. D., Nadin, A., Evin, G., Masters, C. L., Harrison, T., et al. (2001) *J Biol Chem* **276**, 45394–45402
16. Berezovska, O., Jack, C., McLean, P., Aster, J. C., Hicks, C., Xia, W., et al. (2000) *J Neurochem* **75**, 583–593
17. Dovey, H. F., John, V., Anderson, J. P., Chen, L. Z., de Saint Andrieu, P., Fang, L. Y., et al. (2001) *J Neurochem* **76**, 173–181
18. Seiffert, D., Bradley, J. D., Rominger, C. M., Rominger, D. H., Yang, F., Meredith, J. E., Jr., et al. (2000) *J Biol Chem* **275**, 34086–34091
19. Getman, D. P., DeCrescenzo, G. A., Heintz, R. M., Reed, K. L., Talley, J. J., Bryant, M. L., et al. (1993) *J Med Chem* **36**, 288–291
20. Esler, W. P., Kimberly, W. T., Ostaszewski, B. L., Ye, W., Diehl, T. S., Selkoe, D. J., et al. (2002) *Proc Natl Acad Sci USA* **99**, 2720–2725
21. Li, Y. M., Lai, M. T., Xu, M., Huang, Q., DiMuzio-Mower, J., Sardana, M. K., et al. (2000) *Proc Natl Acad Sci USA* **97**, 6138–6143
22. Li, Y. M., Xu, M., Lai, M. T., Huang, Q., Castro, J. L., DiMuzio-Mower, J., et al. (2000) *Nature* **405**, 689–694
23. Blair, S. S. (2000) Imaginal Discs. In *Drosophila Protocols* (Sullivan, W., Ashburner, M., and Hawley, R. S., eds), pp. 159–173, Cold Spring Harbor Laboratory Press, New York
24. Wolfe, M. S., Xia, W., Moore, C. L., Leatherwood, D. D., Ostaszewski, B., Donkor, I. O., et al. (1999) *Biochemistry* **38**, 4720–4727
25. Wolfe, M. S., Xia, W., Ostaszewski, B. L., Diehl, T. S., Kimberly, W. T. and Selkoe, D. J. (1999) *Nature* **398**, 513–517
26. Kimberly, W. T., Xia, W., Rahmati, T., Wolfe, M. S., and Selkoe, D. J. (2000) *J Biol Chem* **275**, 3173–3178

27. Esler, W. P., Kimberly, W. T., Ostaszewski, B. L., Diehl, T. S., Moore, C. L., Tsai, J.-Y., et al. (2000) *Nature Cell Biology* **2**, 428–434
28. Struhl, G., and Greenwald, I. (1999) *Nature* **398**, 522–525
29. Struhl, G., and Adachi, A. (2000) *Mol Cell* **6**, 625–636
30. Ye, Y., Lukinova, N., and Fortini, M. E. (1999) *Nature* **398**, 525–529
31. Shellenbarger, D. L., and Mohler, J. D. (1978) *Dev Biol* **62**, 432–446
32. Micchelli, C. A., Rulifson, E. J., and Blair, S. S. (1997) *Development* **124**, 1485–9145
33. Rulifson, E. J., and Blair, S. S. (1995) *Development* **121**, 2813–2824
34. de Celis, J. F., and Garcia-Bellido, A. (1994) *Mech Dev* **46**, 109–122
35. Klein, T., and Arias, A. M. (1998) *Development* **125**, 2951–2962
36. Phillips, R. G., and Whittle, J. R. (1993) *Development* **118**, 427–438
37. Williams, J. A., Paddock, S. W., Vorwerk, K., and Carroll, S. B. (1994) *Nature* **368**, 299–305
38. Kim, J., Irvine, K. D., and Carroll, S. B. (1995) *Cell* **82**, 795–802
39. Kim, J., Sebring, A., Esch, J. J., Kraus, M. E., Vorwerk, K., Magee, J., et al. (1996) *Nature* **382**, 133–138
40. Rubin, G. M., and Lewis, E. B. (2000) *Science* **287**, 2216–2218
41. Huppert, S. S., Le, A., Schroeter, E. H., Mumm, J. S., Saxena, M. T., Milner, L. A., et al. (2000) *Nature* **405**, 966–970
42. Hadland, B. K., Manley, N. R., Su, D., Longmore, G. D., Moore, C. L., Wolfe, M. S., et al. (2001) *Proc Natl Acad Sci USA* **98**, 7487–7491
43. Doerfler, P., Shearman, M. S., and Perlmutter, R. M. (2001) *Proc Natl Acad Sci USA* **98**, 9312–9317
44. Presente, A., Andres, A., and Nye, J. S. (2001) *Neuroreport* **12**, 3321–3325

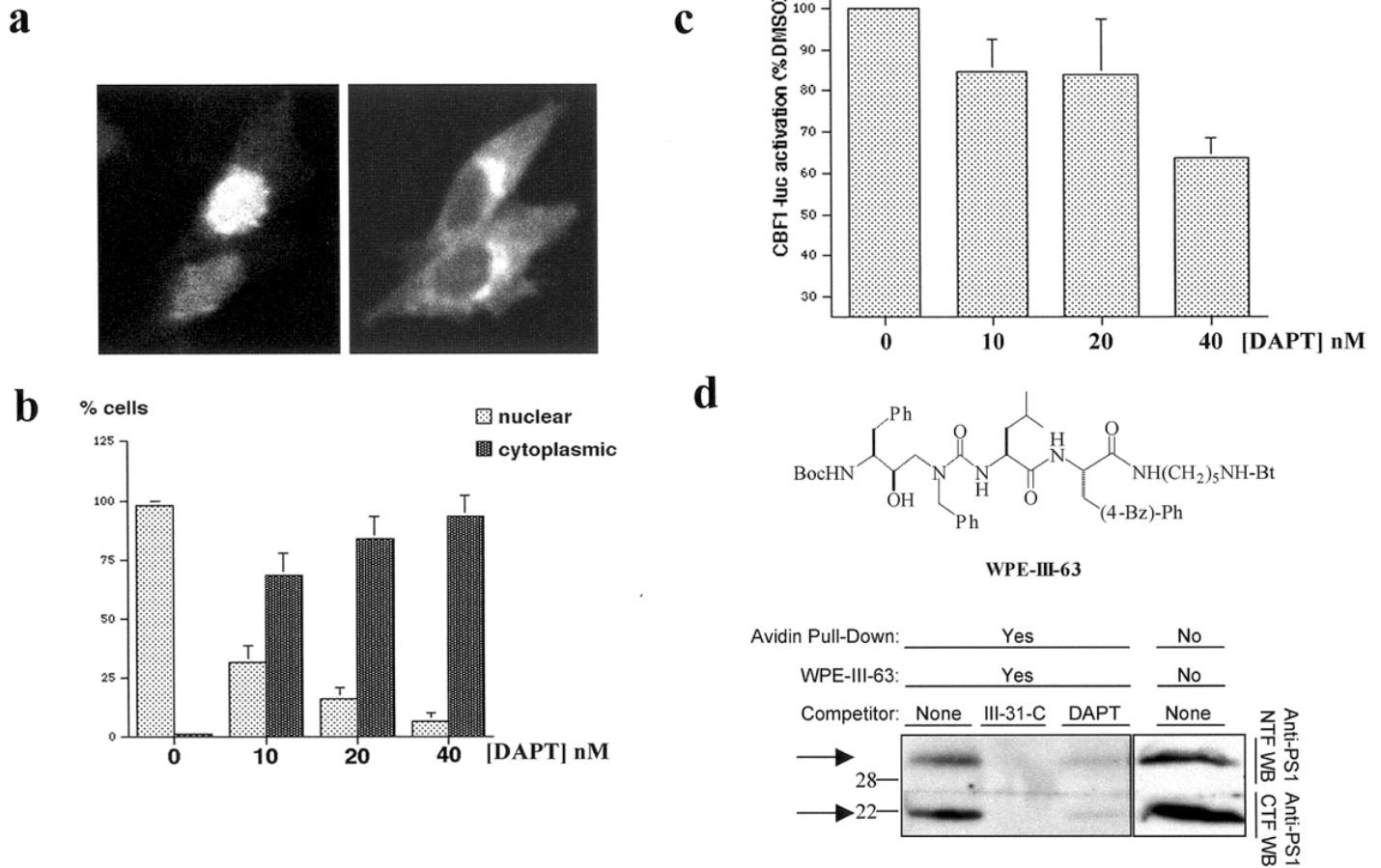
*Received May 23, 2002; accepted September 18, 2002.*

Fig. 1



**Figure 1. *N*-[*N*-(3,5-Difluorophenacetyl)-*L*-alanyl]-(*S*)-phenylglycine *t*-butyl ester (DAPT) inhibits the transmembrane proteolysis of both amyloid- $\beta$  precursor protein (APP) and notch (N). a** APP and N are processed by membrane-tethered proteases that shed their ectodomains and produce membrane-associated C-terminal stubs C99 (from APP) and NEXT (from N). These stubs are substrates for presenilin (PS)-dependent  $\gamma$ -secretase activities. The active site of  $\gamma$ -secretase is apparently at the interface of PS heterodimers, composed of an N-terminal fragment (NTF) and C-terminal fragment (CTF), each subunit contributing a conserved transmembrane aspartate critical for  $\gamma$ -secretase activity. **b** DAPT inhibits cell-free production of A $\beta_{40}$  from the Flag-tagged APP-based substrate C100Flag. Bicarbonate-washed, CHAPSO-solubilized HeLa cell microsomes were incubated with C100Flag for 4 h in the presence of the indicated concentrations of DAPT. **c** DAPT also inhibits the cell-free proteolysis of a N-based substrate, N100Flag. Substrate and product (top and bottom arrow, respectively) were detected by anti-Flag Western blot.

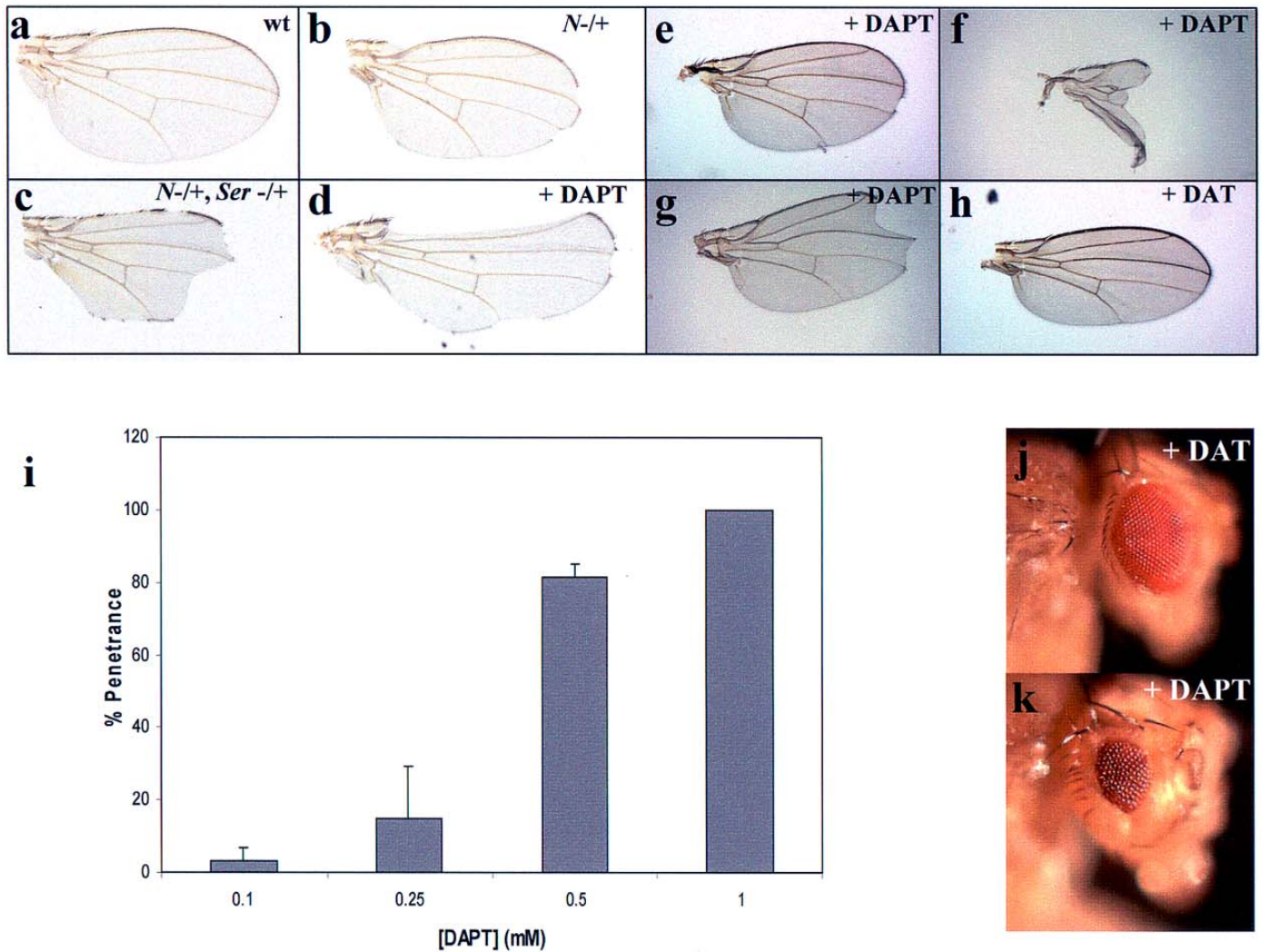
**Fig. 2**



**Figure 2. DAPT inhibits the translocation and signaling of N and blocks photoaffinity labeling of PS heterodimers.** **a)** CHO cells were transiently transfected with a truncated form of N constitutively cleaved by  $\gamma$ -secretase (Notch $\Delta$ E) and fused on the C-terminus with EGFP. Cells were treated 24 h posttransfection with dimethyl sulfoxide (DMSO) vehicle alone (left) or with 40 nM DAPT (right) and visualized after 30 min by fluorescence microscopy. **b)** Quantitation of cells containing nuclear fluorescence (light bars) or cytoplasmic fluorescence (dark bars) after transient transfection with Notch $\Delta$ E-EGFP and treatment as above with varying concentrations of DAPT. **c)** CBF1-luciferase reporter assay. Constitutively cleaved Notch1 $\Delta$ E and the CBF1-luc reporter construct were cotransfected into CHO cells stably expressing human PS1 in the presence of DAPT as indicated. Luc activity was measured 24 h later. Results are shown as a percentage of signal produced from cells treated with vehicle DMSO alone. **d)** Solubilized HeLa cell microsomes were treated with 100 nM of the biotinylated, photoactivatable probe WPE-III-63 in the presence of 20 molar excess of the indicated competitor. After irradiation at 350 nm for 1 h, biotinylated proteins were brought down with streptavidin beads, separated by SDS-PAGE, and analyzed by Western blot, using antibodies specific to the N-terminus or C-terminus of PS1.

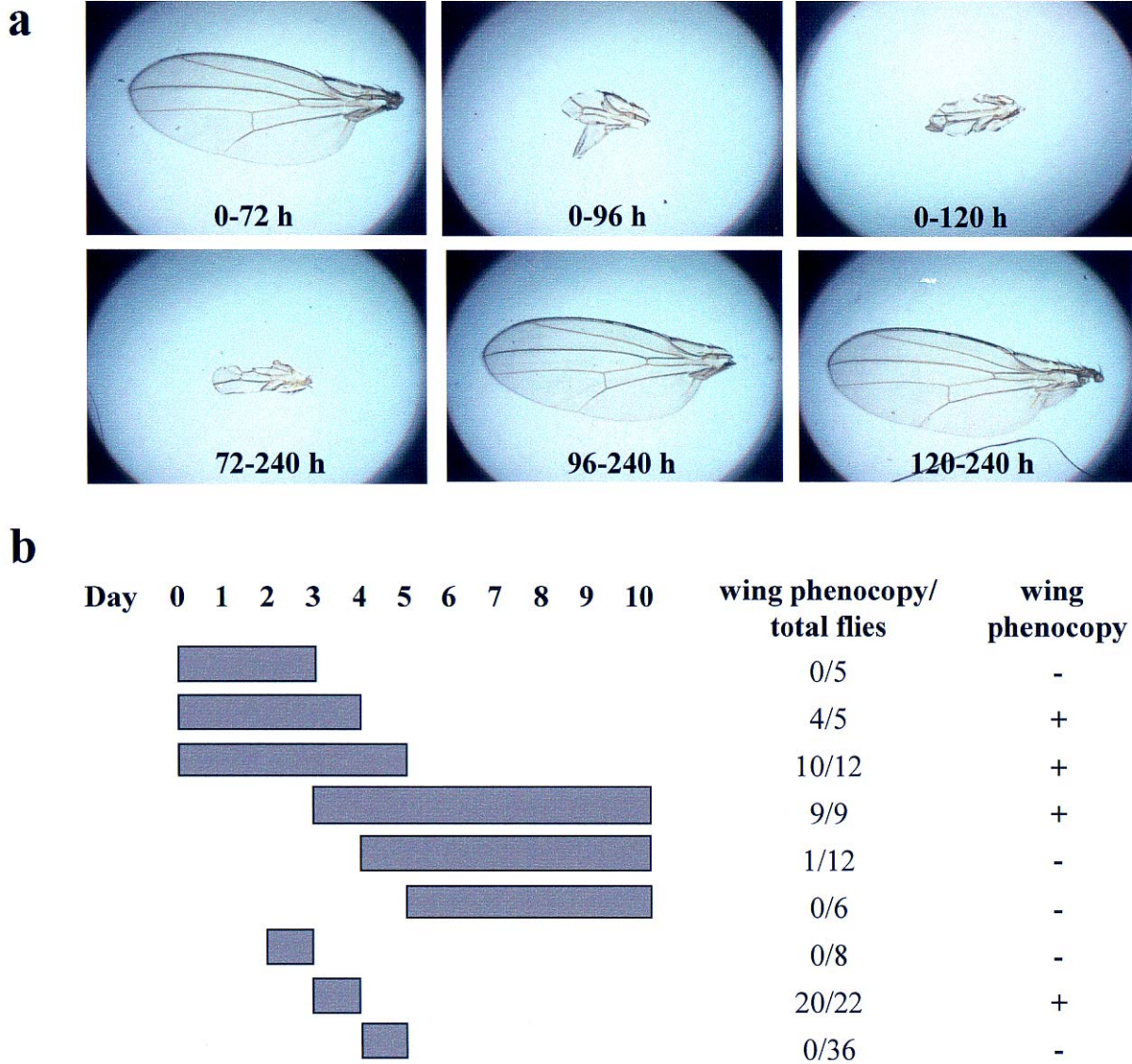


Fig. 3



**Figure 3. Effect of DAPT on *Drosophila* development.** Wings from **a)** wild-type *Drosophila*, **b)**  $N^{55e11/+}$ , and **c)**  $N^{55e11/+}$  and TM3 *Ser*+, **d–g)** wild-type in the presence of 1 mM DAPT, and **h)** wild-type in the presence of 1 mM control compound DAT. **i)** Percent of enclosed flies with the *N* wing phenocopy (i.e., penetrance) after growth in different concentrations of DAPT. **j)** Eyes from wild-type *Drosophila* grown in the presence of 1 mM DAT or **k)** 1 mM DAPT. Adult wings are mounted with anterior at the top.

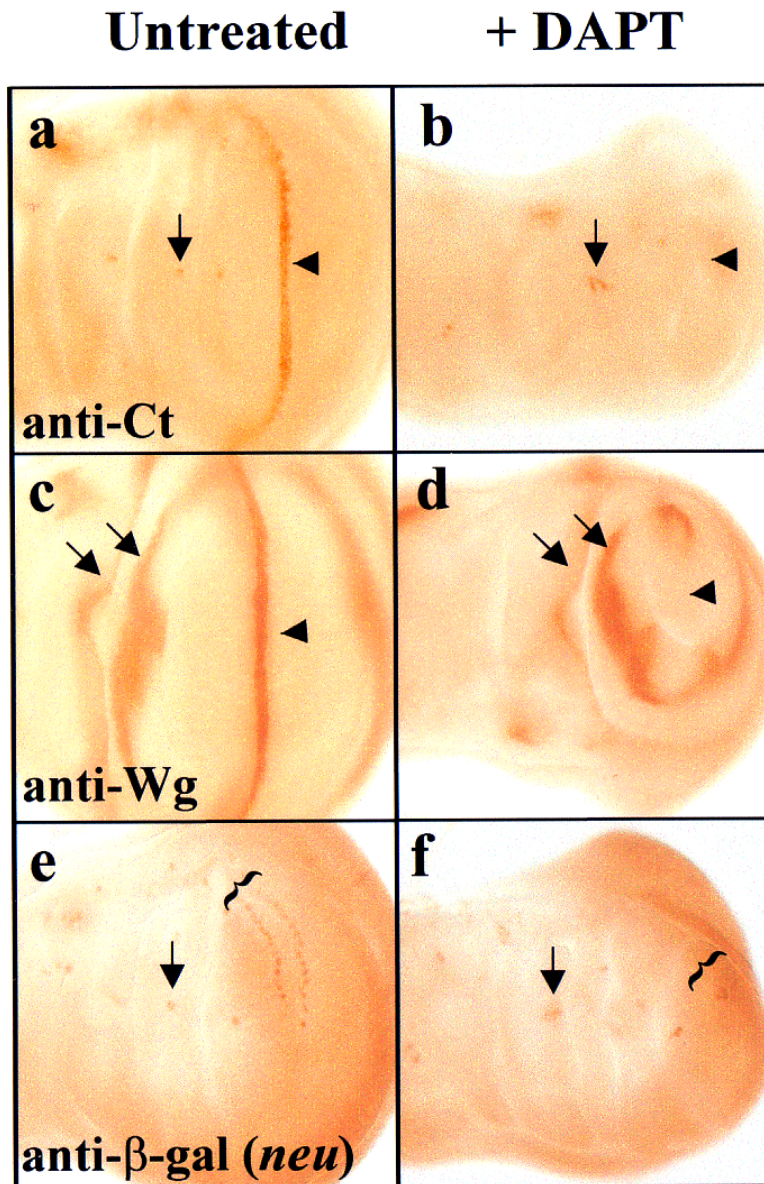
**Fig. 4**



**Figure 4. DAPT affects wing patterning on day 4 of *Drosophila* development. a)** Embryos and larvae were introduced into food containing 1 mM DAPT during the specified periods, and representative wings were taken from the eclosed flies. **b)** The total number of eclosed flies and those with notched wings was determined for each time period of DAPT treatment (gray bars).

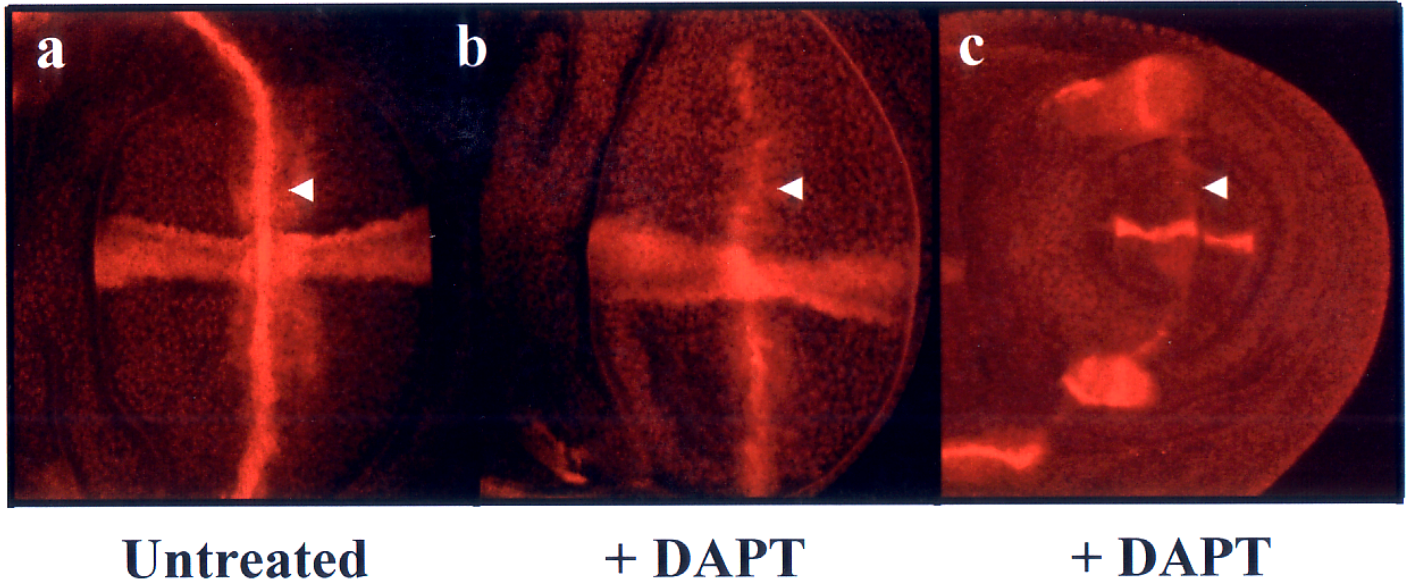


Fig. 5



**Figure 5. DAPT treatment affects *N*-dependent markers in the wing imaginal disc.** Wild-type discs were dissected from untreated third instar larvae (**a**, **c**, and **e**) and from larvae grown in the presence of 1 mM DAPT (**b**, **d**, and **f**). Discs were stained with antibodies against the Ct transcription factor (**a**, **b**), the Wingless ligand (**c**, **d**), and  $\beta$ -gal to detect the expression of the *neu*-LacZ reporter (**e**, **f**). **a**) Ct protein along the presumptive wing margin is *N*-dependent. Arrowhead marks the position of the presumptive wing margin. Arrow marks the position of the giant sensillum of the radius (GSR) SMC. **b**) DAPT treatment leads to a loss of Ct on the margin (arrowhead). Note the extra SMCs detected by anti-Ct (arrow) and the overall reduction in the size of the wing pouch. **c**) Wg protein along the presumptive wing margin is also *N*-dependent (arrowhead). **d**) DAPT treatment leads to a loss of Wg on the margin (arrowhead). Arrows in **c** and **d** mark the rings of Wg around the presumptive wing blade. Note that these rings of expression are not affected by DAPT, although the overall size of the wing pouch is reduced. **e**) Discs dissected from *neu*-LacZ larvae. Bracket denotes two rows of *neu*-expressing cells adjacent to the presumptive anterior wing margin. Arrow marks the position of the giant sensillum of the radius (GSR) SMC. **f**) DAPT-treated disc shows a loss of *neu*-expressing cells along the anterior margin (bracket). Note the neural hyperplasia in the region of the GSR (arrow).

Fig. 6



**Figure 6. DAPT treatment affects *vg* intron 2, a direct transcriptional target of *N*.** **a)** Untreated *vg*-intron 2 LacZ disc. Arrowhead shows *N*-dependent *vg* intron 2 LacZ expression along presumptive wing margin. **b)** *vg* intron 2 LacZ wing disc from a larva treated with DAPT. Arrowhead shows reduction of *vg* intron 2 LacZ expression along the wing margin. **c)** *vg* intron 2 LacZ wing disc treated with DAPT that shows a more severe reduction in *vg* intron 2 LacZ expression along the wing margin. Note that the size of the wing pouch in this disc is reduced, consistent with a strong reduction in *N* signaling. Discs are mounted with anterior at the top.

THE  
**FASEB** JOURNAL

The Journal of the Federation of American Societies for Experimental Biology

**g-Secretase/presenilin inhibitors for Alzheimer's disease  
phenocopy *Notch* mutations in *Drosophila***

Craig A. Micchelli, William P. Esler, W. Taylor Kimberly, et al.

*FASEB J* published online November 1, 2002

Access the most recent version at doi:[10.1096/fj.02-0394fje](https://doi.org/10.1096/fj.02-0394fje)

---

**Subscriptions**

Information about subscribing to *The FASEB Journal* is online at  
<http://www.faseb.org/The-FASEB-Journal/Librarian-s-Resources.aspx>

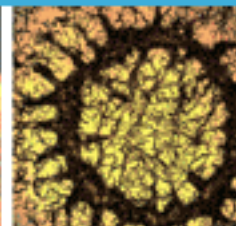
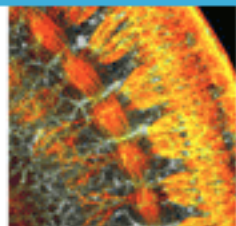
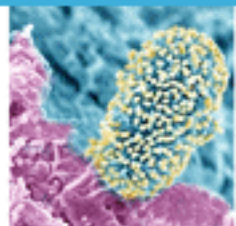
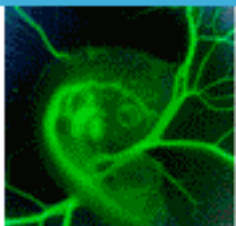
**Permissions**

Submit copyright permission requests at:  
<http://www.fasebj.org/site/misc/copyright.xhtml>

**Email Alerts**

Receive free email alerts when new an article cites this article - sign up at  
<http://www.fasebj.org/cgi/alerts>

---



**Submit  
Image or**